JOURNAL OF AIRCRAFT
Vol. 33, No. 2, March–April 1996

Characteristics of Surface Roughness Associated with Leading-Edge Ice Accretion

Jaiwon Shin*
NASA Lewis Research Center, Cleveland, Ohio 44135

Detailed measurements of surface roughness dimensions associated with leading-edge ice accretions are presented to provide information on characteristics of roughness and trends of roughness development with various icing parameters. Data were obtained from icing tests conducted in the Icing Research Tunnel at NASA Lewis Research Center using a NACA 0012 airfoil. Dimensions measured include diameters, heights, and spacing of roughness elements along with chordwise icing limits. Results confirm the existence of smooth and rough ice zones and that the boundary between the two zones (surface roughness transition region) moves upstream towards stagnation region with time. The heights of roughness elements increase as the total temperature and the liquid water content increase; however, the airspeed has little effect on the roughness height. Results also show that the roughness in the surface roughness transition region grows during a very early stage of accretion, but reaches a critical height and then remains fairly constant. Results also indicate that a uniformly distributed roughness model is only valid at a very early stage of the ice accretion process.

Nomenclature

k = measured roughness height, mm
k_c = critical roughness height inducing a boundary-layer transition, mm
k_s = sand grain roughness height, mm
LWC = liquid water content, g/m^3
MVD = mean volume diameter, μm
s = distance along the surface, mm
t = accretion time, min
V_∞ = airspeed, m/s

Introduction

IT is a well-known fact that iced surfaces develop roughness during an ice accretion process. Surface roughness elements modify the local collection efficiency over the elements themselves and affect local convective heat transfer rates, which in turn affects the overall ice shape. Surface roughness also has an important effect on development of the boundary layer. Despite the importance, there has not been much work done to investigate the surface roughness associated with ice accretion.

With a lack of empirical correlations that can be used to evaluate the effect of roughness elements found on typical ice accretions, it has become standard practice in current ice accretion prediction methods to develop an empirical correlation for either the surface element roughness height or the convective heat transfer coefficient. These correlations are developed by first predicting the ice shapes for a set of experimental ice shapes by changing the roughness element height (or the convective heat transfer coefficient) to determine the value that yields the best agreement with experiment.

This type of approach raises several concerns. First, empirical correlations developed by this approach do not reflect ice accretion physics or actual surface conditions, and they are dependent on the numerical algorithm. Secondly, these empirical correlations relate the sand grain roughness height to the icing parameter, using the concept of equivalent sand grain roughness stemming from the work of Nikuradse[1] and Schlichting.[2] Although this type of roughness has been widely used for many applications in fluid mechanics and a large amount of experimental data is available, surface roughness characteristics associated with ice accretions are very different from conventional roughness types such as the sand grain roughness in both size and distribution. These concerns precipitated a need for development of a better physical roughness model for ice accretion prediction methods.

For the development of a better physical roughness model, there have been several studies[3–6] to increase an understanding of the surface roughness physics. However, previous studies have dominantly been observational and qualitative through the use of close-up photography or videography. To understand the roughness effects on the boundary layer, detailed boundary-layer measurements are necessary over the iced surface with realistic roughness. However, there has not been any work providing quantitative data describing size and distribution of roughness for boundary-layer measurement tests to use. The objective of the current study is to fill this gap and bring more insights for roughness model development efforts.

Test Method

Test Model

To eliminate any geometry-related variation in roughness characteristics for this investigation, a single airfoil was used for all testing. The airfoil had a 0.53-m (21-in.) chord and a 1.83-m (6-ft) span with a cross section of a NACA 0012 airfoil. The model was set at a 0-deg angle of attack for the entire test.

Test Conditions

Test conditions were selected to study the effects of airspeed, air temperature, LWC, and accretion time on the surface roughness. The conditions were chosen mainly to produce glaze ice since roughness and heat transfer are much more important in the glaze ice regime. For this reason, tests were conducted mostly near the freezing point.

Presented as Paper 94-0799 at the AIAA 32nd Aerospace Sciences Meeting and Exhibit, Reno, NV, Jan. 10–13, 1994; received June 24, 1994; revision received Sept. 22, 1995; accepted for publication Sept. 22, 1995.

*Aerospace Engineer, Icing Technology Branch, Propulsion Systems Division; currently Deputy Project Manager, High Speed Research Propulsion Project Office. Member AIAA.

Table 1 Measured roughness size for effects of icing parameters

	Height, mm	Diameter, mm	Spacing, mm	Width of smooth, zone, mm
Airspeed, m/s				
67.1	0.57 (0.01)	1.11 (0.20)	1.28 (0.14)	6.0
89.5	0.58 (0.07)	1.05 (0.11)	1.28 (0.07)	5.0
111.8	0.58 (√)	1.06 (0.12)	1.19 (0.09)	4.0
Total temperature, °C				
−1.1	0.62 (0.09)	1.33 (0.27)	1.45 (0.17)	8.0
−2.2	0.57 (0.01)	1.11 (0.20)	1.28 (0.14)	6.0
−3.9	0.51 (0.06)	0.93 (0.11)	1.02 (0.25)	6.0
LWC, g/m^3				
0.5	0.57 (0.01)	1.11 (0.20)	1.28 (0.14)	6.0
0.75	0.61 (√)	1.22 (0.18)	1.48 (0.11)	5.5
1.0	0.74 (0.04)	1.42 (0.16)	1.59 (0.23)	5.0
1.2	0.79 (0.07)	1.56 (0.19)	1.71 (0.04)	4.5

A symbol √ indicates a data point with a bad height image. Height information is inferred from the diameter measurement.
Numbers in parentheses for height, diameter, and spacing are standard deviations.

Data Acquisition Method

There were three requirements for the data acquisition method to meet the objective of the test.

1) The method should be able to provide detailed and accurate enough data for measurements of the roughness element size which is on the order of a millimeter.

2) The method should be able to provide fast acquisition and processing capabilities to handle a large size database for studying the trend of roughness characteristics with icing parameters.

3) The method should not alter the surface condition during a data acquisition process. Given these requirements, an optical imaging technique was chosen over mechanical measurement techniques. Each iced surface was photographed using a Kodak digital camera system with a 60-mm macrolens to capture detailed surface roughness characteristics. The resolution of the camera is 1024 × 1280 pixels. Images were later transmitted to a personal computer for measurements. Actual measurements of roughness elements were done using an image processing program. In addition to digital images, ice shapes and section drag were documented.

Two types of digital images were taken to capture both base and height dimensions of roughness elements. For diameter and spacing measurements the lens was aimed normal to the surface to obtain a plan view. For height measurements the lens was aimed parallel to the surface to reveal the profile of roughness elements.

Results and Discussions

A majority of measurements for the roughness size were made in the region where the rough zone begins downstream of the smooth zone. This region will be referred to as the surface roughness transition region because it is the region where surface condition changes from a smooth one to a rough one. The results from this region are used to study icing parameter effects and accretion time effects on the roughness size. Reasons for selecting this surface location for the measurements will be discussed later after the results are presented.

Effects of Icing Parameters

The results in this section present roughness size measurements for various airspeeds, air temperatures, and LWCs to illustrate the effects of these icing parameters on the roughness size. All data are for 2-min ice accretions.

The height, diameter and spacing of roughness elements were measured for three airspeeds (67.1, 89.5, and 111.8 m/s), three air temperatures (−1.1, −2.2, and −3.9°C in total temperature), and four LWCs (0.5, 0.75, 1.0, and 1.2 g/m^3). For each dimension, a number of measurements were made to obtain a mean value. The mean values and standard deviations of the diameter, height, and spacing are listed in Table 1. Also included is the width of smooth zone that is measured from the stagnation line to the beginning of the rough zone. Roughness elements are hemispheres unless otherwise noted.

In Fig. 1, measured roughness height is plotted vs airspeed, total temperature, and LWC. (Roughness values predicted by the ice roughness correlation recommended for use with the LEWICE code in the LEWICE User's Manual[7] are included in the figures; only comparison of trends is meaningful in these figures since the roughness correlation provides an equivalent sand grain roughness height, not an actual roughness height.) Trends are the same between the measured roughness height and the LEWICE predicted height, except for the airspeed. The current results show almost constant roughness height with increasing airspeed, whereas the LEWICE roughness model predicts growth of the roughness height with airspeed. One other noteworthy observation is that for the effect of LWC, the growth rate of the roughness height predicted by the LEWICE model is much higher than the one suggested by the current result.

Comparison of Measured Roughness Heights to Calculated Boundary-Layer Thickness and Critical Roughness Heights

Figure 2 shows comparisons of the measured roughness height with the predicted laminar boundary-layer thickness and with the predicted critical roughness height to cause a transition. Bragg et al. calculated the boundary-layer thickness and critical roughness heights shown in the figure using the ISES computer code, and their method is described in detail in Ref. 8. The boundary-layer thickness results are for a clean NACA 0012 airfoil and the critical roughness height was calculated based on an assumption that the boundary-layer transition occurs because of the presence of a single hemisphere at each plotted location. The figure indicates that if the roughness height is bigger than the critical roughness height at a given surface location, a transition is likely to occur. Also plotted are the measured roughness heights at surface locations where these measurements were made, namely the beginning of the rough zone.

As mentioned, the boundary-layer thicknesses in Fig. 2 are for a clean airfoil, and so they do not account for geometry changes at the leading edge made by 2-min ice accretions or effects caused by surface roughness. However, for small ice accretions with no horns such as the ones used here, a geometry change because of an ice accretion near the stagnation region would be very close to outward displacement of the airfoil leading edge. Also, the boundary layer would develop over a fairly smooth iced surface until it reaches the surface roughness transition region where roughness starts to form and where the measurements were made. Therefore, a clean airfoil boundary-layer thickness may be used as an acceptable esti-

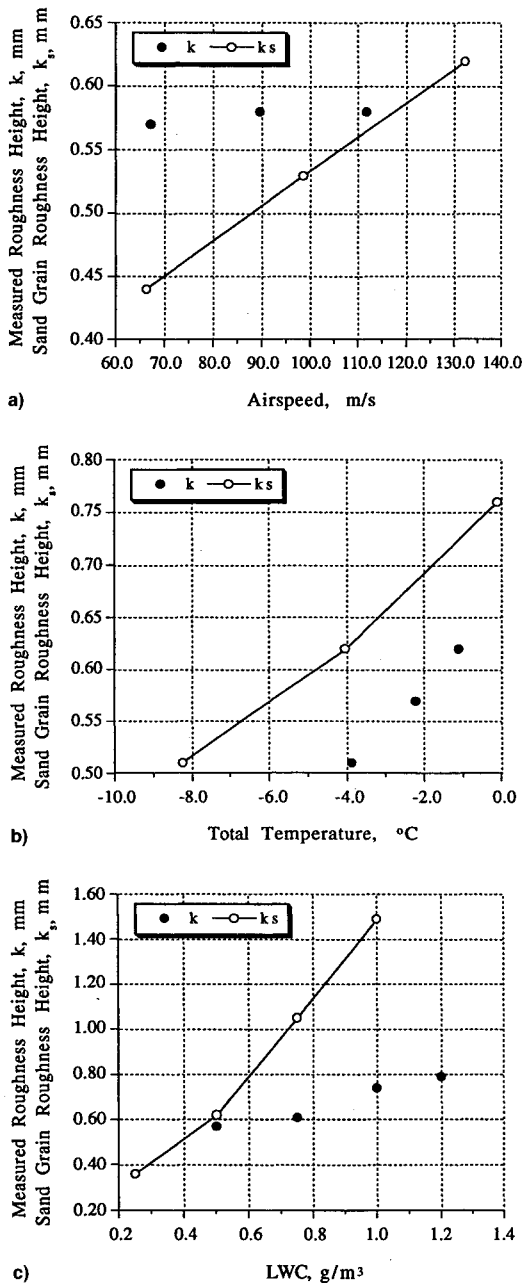

Fig. 1 Comparison of k with k_s, predicted by LEWICE roughness model: a) airspeed, b) total temperature, and c) LWC.

mate for a boundary-layer thickness over the surface of a small ice accretion near the stagnation region. Critical roughness heights were calculated based on a single roughness element, which is totally different from the roughness characteristic of the current study. Calculated critical roughness heights are meant to be used to get a rough idea about a roughness height for a boundary-layer transition.

As can be seen, roughness heights in all cases are much higher than the boundary-layer thickness and critical roughness heights, implying that roughness elements at measurement locations might cause a transition. Whether this height indeed causes a transition needs to be investigated further through detailed boundary-layer measurements with the same roughness size and spacing. Note that the boundary-layer thickness and the critical roughness height become smaller with increasing airspeed, which makes a constant roughness height bigger relative to the boundary-layer thickness (Fig. 2).

In Fig. 2, measured roughness heights are plotted at the beginning of the rough zone for each icing condition. Therefore, information on the width of the smooth zone can be obtained from these surface locations where measured roughness heights are plotted. It can be seen that at colder temperatures, increasing airspeed and increasing LWC move the beginning of the rough zone closer to the stagnation region. These findings are consistent with earlier findings by Hansman et al.[4] on a cylinder.

Effects of Accretion Time

In this section, measurement results of the roughness height, diameter, and spacing are presented at several accretion times to study roughness development with time. Measured values are listed in Table 2. As a base case, a glaze ice condition with a moderate LWC (0.5 g/m^3) and MVD (20 μm) at the airspeed of 67.1 m/s and the air temperature of -2.2°C was tested for 1, 2, 3, and 6 min. Two other conditions for a higher airspeed and a higher air temperature were tested to make a comparison with the base icing condition. For these two conditions, only 2- and 6-min ice accretions were available for the measurement.

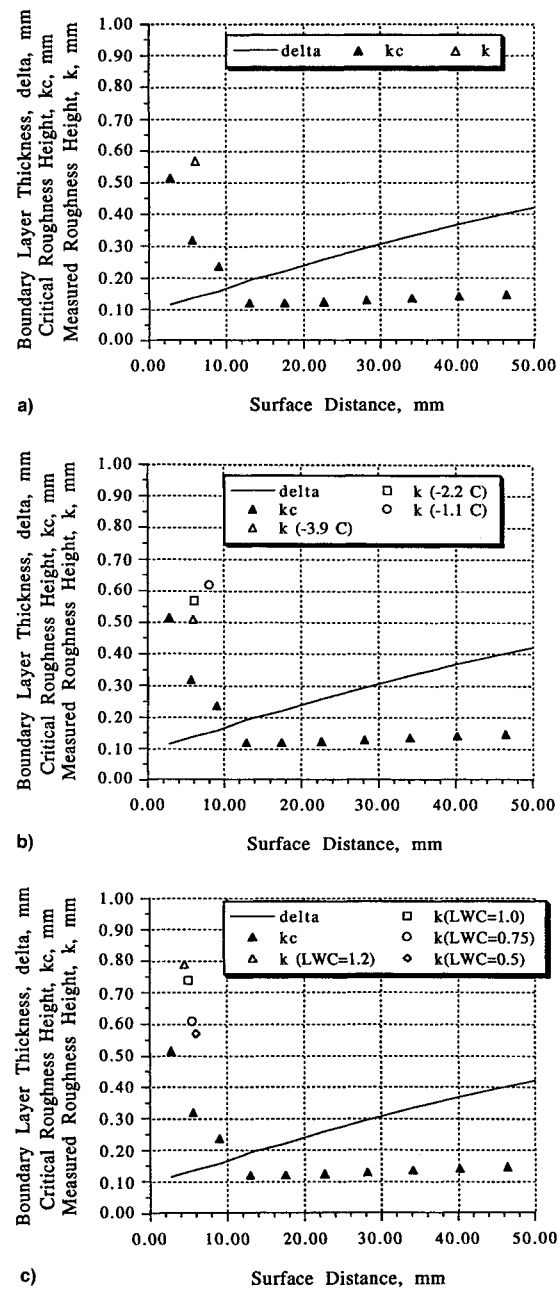

Fig. 2 Comparison of measured roughness height with boundary-layer thickness and critical roughness height: a) V_∞ = 67.1 m/s, b) temperature effect, and c) LWC effect.

Table 2 Measured roughness size for effects of accretion time

Accretion time, min	Height, mm	Diameter, mm	Spacing, mm	Width of smooth zone, mm
Base condition (V_∞ = 67.1 m/s; total temperature = −2.2°C)				
1	0.28 (0.06)	0.56 (0.07)	0.56 (0.07)	7.0
2	0.57 (0.01)	1.11 (0.20)	1.28 (0.14)	6.0
3	0.62 (0.03)	1.15 (0.11)	1.33 (0.14)	6.0
6	0.55 (0.08)	1.05 (0.11)	1.18 (0.11)	3.5
Higher airspeed (V_∞ = 111.8 m/s; total temperature = −2.2°C)				
2	0.58 (√)	1.06 (0.12)	1.19 (0.09)	4.0
6	0.57 (0.05)	1.15 (0.07)	1.32 (0.11)	0.0
Higher total temperature (V_∞ = 67.1 m/s; total temperature = −1.1°C)				
2	0.62 (0.09)	1.33 (0.27)	1.45 (0.17)	8.0
6	0.63 (0.04)	1.21 (0.11)	1.39 (0.14)	5.0

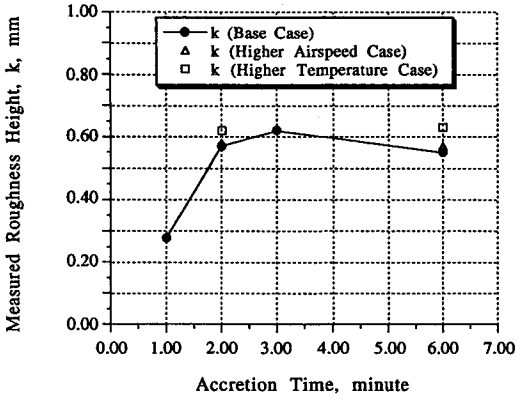

Fig. 3 Effects of accretion time on roughness height.

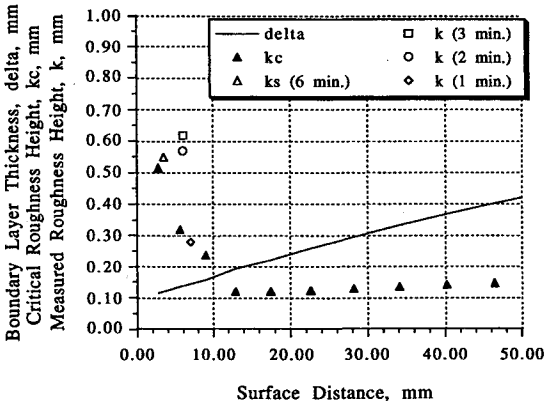

Fig. 4 Comparison of measured roughness height with boundary layer.

Figure 3 shows roughness heights of the three icing conditions at various accretion times. Measurements were all made at the surface roughness transition region. As can be seen with the base case, the height grows quite rapidly during the first 2 min, then very slowly between 2–3 min, and the height decreases slightly after 3 min. The other two icing conditions also show either no change or a slight increase in the height between 2–6 min. It appears that there are definitely two different growth rates: 1) a rapid growth rate during the early stage and 2) a very slow or even possibly a zero rate during the later stage of the ice accretion process. This result is contradictory to the popular view of continuous growth of roughness size with time.

Figure 4 shows the roughness heights of the base case at all four accretion times plotted with the boundary-layer thickness

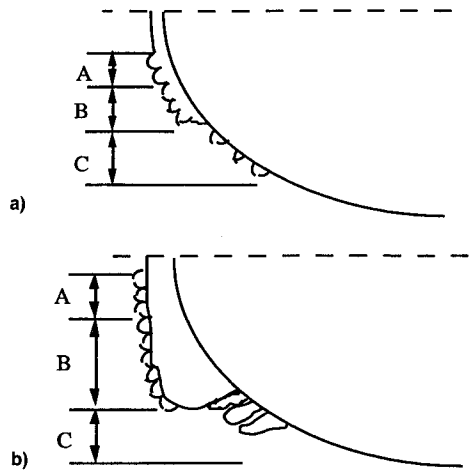

Fig. 5 Illustration of ice shape and roughness growth: a) initial and b) horn growth stage.

and the predicted critical roughness height for a transition. It shows that roughness at 1 min protrudes above the boundary layer, but it has not quite grown out of the predicted critical roughness height, whereas the roughness heights at 2 and 3 min are well above the boundary-layer thickness and the critical roughness height. Another important observation is that the rough zone hardly moved toward the stagnation region between 1–3 min, although the roughness height continued to grow. Based on these two observations, it is plausible to assume that an onset of the physical mechanism that moves the rough zone toward the stagnation region occurs after the roughness reaches a critical height, which is significantly higher than the boundary-layer thickness (in this case about four times higher than the boundary-layer thickness), and once this mechanism takes place, roughness grows much slower or stops growing as discussed earlier. This finding provides useful guidance for future studies to understand roughness development at the surface roughness transition region and its interaction with the boundary layer. One could also utilize this information to estimate a roughness height at any time during a very early stage of an ice accretion by interpolating the heights at the zero time and at the time when the height growth slows down or stops.

Qualitative Description of Glaze Ice Accretion Process Based on Digital Images

There were several reasons for selecting the surface roughness transition region for the measurements. First, it is a very important region in terms of roughness and boundary-layer development. One of the questions that has precipitated many discussions is what causes a distinct difference in the surface condition in this region. One of the theories (Ref. 4) is that a water film forms stationary beads because of surface tension causing a transition in the boundary layer, which enhances heat transfer and freezes the water beads. Although it is plausible, there has not been any investigation to find whether a boundary-layer transition indeed takes place at the beginning of the rough zone. To address this question, it is necessary to make detailed boundary-layer measurements over a rough surface with the same kind of surface condition as an actual ice accretion. For this, it is essential to understand the roughness characteristics in this region. Secondly, it was found during the data analysis that the roughness size does not change along the surface in the rough zone. Therefore, it was not a concern where measurements need to be made.

Having stated that roughness size remains unchanged in the rough zone, more discussion is necessary to understand the definitions of roughness and the rough zone used in the current study. Olsen and Walker[3] observed that roughness grows with time, which is found to be true from the results of this study,

Table 3 Measured roughness size for roughness characteristics along the surface

	Glaze ice		Rime ice	
	2-min ice accretion	6-min ice accretion	2-min ice accretion	6-min ice accretion
Width of smooth zone, mm	6	3.5	5.0	5.0
Height at surface roughness transition region, mm	0.57	0.55	0.17	0.21
Height at horn region, mm	0.57(‡)	0.64(‡)	NA	NA
Mean feather height, mm	1.20	2.3	2.45	7.04
Feather height range, mm	1.09–1.38	1.68–3.42	2.05–2.85	6.28–7.80
Feather growth direction	Normal to the flow	Normal to the flow (right behind the horn) and parallel to the flow (further downstream)	Parallel to the flow	Parallel to the flow
Icing limit, mm	20–25	30–35	NA	NA

A symbol ‡ indicates that height information is inferred from diameter measurements because of unavailable height images. NA denotes data not available.

at least until a critical roughness size is reached. However, digital images show that there are two types of growth. One is macrogrowth responsible for forming a main ice shape with horns and feathers. The other is microgrowth responsible for forming roughness on the surface of the macroice shape. An illustration of roughness and ice shape development is given in Fig. 5. At the initial stage of an ice accretion (Fig. 5a), roughness develops on an ice substrate that has a fairly uniform thickness (see regions A and B). Small ice bumps at various spots grow aft of the rough zone (region C) in what is commonly referred to as a feather region. In the feather region, there is no ice substrate.

As the ice accretion process continues (Fig. 5b) the rough zone propagates toward the stagnation region and the roughness size at the surface roughness transition region (region A) grows to a critical size as discussed earlier. Roughness elements in region B continue to grow, eventually forming a major ice structure commonly referred to as a horn. The horn grows to have its own hills and valleys along the span, however, these hills and valleys are much bigger in size compared to the roughness in the surface roughness transition region. As this major horn structure develops, roughness elements whose size is almost the same as roughness elements in the surface roughness transition region develop on the horn surface. This phenomenon has not been revealed until digital images with high magnification of the current study showed detailed surface conditions and the measurement technique provided an ability to quantify the roughness size. Feathers in region C also continue to grow with time. Some feathers near the horn merge into the main ice structure adding mass and altering the ice shape, and feathers further downstream grow individually, although they may merge with each other forming a bigger feather. Regardless of where these feathers grow and how they merge together, an ice substrate does not develop in the feather region. Also, the size of these feathers is an order of magnitude bigger than the roughness size in the regions A and B.

These findings and observations clearly suggest that macroirregularity of the horn surface and feather growth should not be considered as roughness, rather they need to be considered as part of an overall ice shape that needs to be calculated in the ice accretion model. The definition used for roughness during this study is that roughness is surface irregularity growing on top of the macroice shape. Also, the definition of the rough zone for the current study is the region where the roughness exists as illustrated in the regions A and B in Fig. 5. It is also apparent that investigations are needed to understand how small initial roughness elements in region B grow to form a large horn structure, and to understand how small roughness elements develop on the horn surface.

Quantitative Comparison of Roughness Characteristics of Glaze and Rime Ice Accretions

As mentioned in the Introduction, the study of ice roughness has another importance in providing information about surface characteristics for aerodynamic tests with simulated ice shapes. For this, detailed documentation of all surfaces of the ice accretion must be obtained. This kind of documentation also provides an understanding of how the surface condition changes during an ice accretion process. A glaze ice accretion and a rime ice accretion are presented to illustrate the obvious difference between the two in accretion physics and the surface condition. The results are presented for 2- and 6-min accretions for a comparison of the surface condition with time.

Measurements were made at the surface roughness transition region, horn area, and the feather region and measured mean values are listed in Table 3. Since digital images for height measurements at the horn area were not available, height information at the horn area is inferred from diameter measurements. Mean values of the feather height for the glaze ice accretions are all measured where feathers grow normal to the surface, However, because of rime feather growth pattern, mean values presented in Table 3 for rime feathers simply represent the length of the feather growing into the local flow direction.

Also, it should be noted that the feather height or length was measured from the airfoil surface, whereas roughness height at the surface roughness transition and horn regions were measured from the top of the ice substrate. It is apparent that feathers are much bigger in size than roughness, which confirms the earlier discussion of the definition of roughness vs ice shape.

It is known that friction drag dominates the airfoil drag with a small ice accretion where surface roughness affects the boundary layer. However, with a bigger ice accretion with horns, pressure drag dominates the airfoil drag by changing the pressure distribution around the leading edge. Ice accretion codes available to date do not account for feather growth and its contribution to the horn growth. Therefore, if an ice shape predicted by these ice accretion codes is used for calculating aerodynamic degradation, effects due to the presence of the feather structure are ignored. With the current observation of the surface condition, it is plausible that the aerodynamic degradation due to the feather structure can be significant, and this might explain why previous studies[9,10] predicted lower airfoil drag compared with the measured drag for large glaze ice shapes.

Concluding Remarks

Characteristics of surface roughness associated with leading-edge ice accretions have been presented. The results were analyzed for the effects of icing parameters and the effect of accretion time. Major findings are as follows:

1) The roughness height increases with increasing temperatures and LWC. These results show the same trend as the current LEWICE sand grain roughness model predicts.

2) The airspeed has little effect on the roughness height; however, roughness height relative to the boundary-layer thickness increases with increasing airspeed as the thickness of the boundary layer decreases.

3) Colder temperatures, increasing airspeed, and increasing LWC move the beginning of the rough zone closer to the stagnation region.

4) Measured roughness heights with 2-min ice accretions are 3–5 times larger than calculated clean airfoil boundary-layer thicknesses at the surface roughness transition region. Although calculated boundary-layer thicknesses are based on somewhat different leading-edge geometry and surface conditions, a magnitude of measured roughness heights suggests that roughness elements at the surface roughness transition region probably protrude well out of the boundary layer and possibly cause a boundary-layer transition.

5) It is found that the roughness growth rate can be quite different between an initial stage and a later stage of an accretion process. The current result suggests rapid initial growth followed by much slower growth or possibly zero growth.

6) It is found that roughness develops on the surface of horn structure that has its own macrosurface irregularity. The relation between the macroice shape growth and microroughness growth needs to be explored further. Feather structure downstream of the horn area should be considered as part of the macroice shape, and irregular surface conditions because of the feather growth need to be accounted for by the ice accretion model, not by a roughness model.

The analyses of roughness heights, boundary-layer thicknesses, and predicted critical roughness heights conducted by the current study suggest a boundary-layer transition occurring at the boundary between the smooth and the rough zones. However, a definite conclusion is not possible because of the use of a clean surface condition and a simpler roughness characteristic for calculating boundary-layer thicknesses and critical roughness heights. To understand the underlying physics, thorough investigation is needed through detailed and carefully devised boundary-layer measurements over realistic rough surfaces. Results from such tests are believed to be able to answer the question of what fixes the roughness and allows it to grow outward and toward the stagnation region.

References

[1]Nikuradse, J., "Strömungsgesetze in Rauher Rohen," VDI-Forschungsheft 361, 1933; also "Laws of Flow in Rough Pipes," NACA TM-1292.

[2]Schlichting, H., "Experimentelle Untersuchungen zum Rauhigkeitsproblem," *Ingenieur-Archiv VII*, Vol. 1, 1936, pp. 1–34; also "Experimental Investigation of the Problem of Surface Roughness," NACA TM-823.

[3]Olsen, W., and Walker, E., "Experimental Evidence for Modifying the Current Physical Model for Ice Accretion on Aircraft Surfaces," NASA TM 87184, May 1986.

[4]Hansman, R. J., Yamaguchi, K., Berkowitz, B., and Potapczuk, M., "Modeling of Surface Roughness Effects on Glaze Ice Accretion," AIAA Paper 89-0734, Jan. 1989.

[5]Hansman, R. J., "Analysis of Surface Roughness Generation in Aircraft Ice Accretion," AIAA Paper 92-0298, Jan. 1992.

[6]Hansman, R. J., Breuer, K. S., Hazan, D., Reehorst, A., and Vargas, M., "Close-Up Analysis of Aircraft Ice Accretion," AIAA Paper 93-0029, Jan. 1993.

[7]Ruff, G. A., and Berkowitz, B. M., "Users Manual for the NASA Lewis Ice Accretion Code (LEWICE)," NASA CR 185129, 1990.

[8]Bragg, M. B., Kerho, M., and Winkler, J., "Effect of Initial Ice Roughness on Airfoil Aerodynamics," AIAA Paper 94-0800, Jan. 1994.

[9]Shin, J., Berkowitz, B., Chen, H., and Cebeci, T., "Prediction of Ice Shapes and Their Effect on Airfoil Performance," AIAA Paper 91-0264, Jan. 1991.

[10]Potapczuk, M., and Al-Khalil, K. M., "Ice Accretion and Performance Degradation Calculations with LEWICE/NS," AIAA Paper 93-0173, Jan. 1993.